Catalytic Oxidation of Carbon Monoxide on Monodispersed Platinum Clusters: Each Atom Counts

U. Heiz,* A. Sanchez, S. Abbet, and W.-D. Schneider

Contribution from the Institut de Physique de la Matière Condensée, Université de Lausanne, CH-1015 Lausanne, Switzerland

Received October 14, 1998

Abstract: Nanoclusters open fascinating opportunities for quantum engineering because quantum-size effects become dominant in determining catalytic,[1-3] optical,[4] electronic,[5] and magnetic[6] properties. We succeeded in the controlled production of low-energy and high-flux monodispersed cluster beams, which allow for a systematic study of their reactivity after deposition onto a chemically inert substrate. We investigated *the* catalytic reaction that is the oxidation of CO on platinum and observed a distinct atom by atom size dependency for monodispersed platinum clusters on thin MgO(100) films. These results clearly show that the efficiency of a heterogeneous catalytic reaction can be tuned by the judicious choice of particle size.

1. Introduction

One of the aims in heterogeneous catalysis is the understanding of the observed catalytic behavior of supported metal particles on a molecular level to optimize the efficiency and selectivity of industrial catalysts. Since the early days of cluster science it has been speculated that a strong size-dependent catalytic activity of metal clusters just a few or few tens of atoms in size exists. This would allow tuning the catalyst's reactivity and selectivity by simply changing the cluster's size. In this way the electronic levels, steric effects, and symmetry of the cluster can be adjusted to obtain the desired resonances between the electronic levels of the catalyst and the molecules involved in the catalytic reaction. However, there still exists no direct experimental proof that model catalysts made of such small clusters indeed reveal such variations in the catalytic activity when cluster size is changed just by single atoms. Promising results pointing toward such an ability have been obtained using gas-phase clusters where size-dependent adsorption of small molecules has been observed.[2,7-10] In a recent study, Shi et al. even investigated a whole catalytic cycle and reported on the size-dependent catalytic oxidation of CO on free Pt_n ($n = 3-6$) clusters in a molecular beam experiment.[11] For supported clusters, Fayet et al.[1] and later Leisner et al.[12] showed that the

latent-image generation in the photographic process requires silver clusters of a critical size. Xu et al. observed a size-dependent catalytic activity of supported metal clusters for the hydrogenation of toluene by using organometallic precursors.[3] In a recent work we showed that the dissociation of CO on size-selected supported nickel clusters is strongly dependent on the exact cluster size,[13] as previously shown in the *gas phase* by Vajda et al.[14] In the size domain, where the particles consist of several hundreds of atoms, the catalytic activity was investigated on size-distributed metal particles.[15,16] An unusual catalytic activity for the oxidation of CO can be observed for nanometer-size gold particles,[17] and it was shown that the onset of the catalytic activity occurs when one dimension of the particle becomes smaller than three atomic spacings.[18]

In this work we went a step further and studied one of the most important catalytic reactions, the oxidation of poisonous CO on model catalysts consisting of monodispersed size-selected platinum clusters deposited on carefully prepared oxide films. The conversion of CO and O_2 into CO_2 in the gas phase has a free enthalpy of -280 kJ/mol and is therefore thermodynamically allowed. However, to initiate this reaction, the activation energy for the dissociation of O_2 has to be overcome, and it is the task of the catalyst to reduce this energy. Studies on single crystals, on supported particles as well as on real catalysts, revealed many details about this catalytic process. On highly coordinated Pt atoms, like on a Pt(111) single crystal, carbon monoxide can be oxidized at low temperature (160 K).[19-21] In

(1) Fayet, P.; Granzer, F.; Hegenbart, G.; Moisar, E.; Pischel, B.; Wöste, L. *Phys. Rev. Lett.* **1985**, *55*, 3002.

(2) Whetten, R. L.; Cox, D. M.; Trevor, D. J.; Kaldor, A. *Phys. Rev. Lett.* **1985**, *54*, 1494.

(3) Xu, Z.; Xiao, F.-S.; Purnell, S. K.; Alexeev, O.; Kawi, S.; Deutsch, S. E.; Gates, B. C. *Nature* **1994**, *372*, 346–348.

(4) Alivisatos, A. P. *Science* **1996**, *271*, 933–937.

(5) Knight, W. D.; Clemenger, K.; de Heer, W.; Saunders: W. A.; Chou, M. Y.; Cohen, M. L. *Phys. Rev. Lett.* **1984**, *52*, 2141.

(6) Billas, I. M. L.; Châtelain, A.; de Heer, W. A. *Science* **1994**, *265*, 1682.

(7) Holmgren, L.; Andersson, M.; Rosén, A. *Surf. Sci.* **1995**, *331–333*, 231–236.

(8) Bérces, A.; Hackett, P. A.; Lian, L.; Mitchell, S. A.; Rayner, D. M. *J. Chem. Phys.* **1998**, *108*, 5476–5490.

(9) Parks, E. K.; Nieman, G. C.; Kerns, K. P.; Riley, S. J. *J. Chem. Phys.* **1998**, *108*, 3731–3739.

(10) Schulze Icking-Konert, G.; Handschuh, H.; Ganteför, G.; Eberhardt, W. *Phys. Rev. Lett.* **1996**, *76*, 1047–1050.

(11) Shi, Y.; Ervin, K. M. *J. Chem. Phys.* **1998**, *108*, 1757–1760.

(12) Leisner, T.; Rosche, C.; Wolf, S.; Granzer, F.; Wöste, L. *Surf. Rev. Lett.* **1996**, *3*, 1105–1108.

(13) Heiz, U.; Vanolli, F.; Sanchez, A.; Schneider, W.-D. *J. Am. Chem. Soc.* **1998**, *120*, 9668–9671.

(14) Vajda, S.; Wolf, S.; Leisner, T.; Busolt, U.; Wöste, L. *J. Chem. Phys.* **1997**, *107*, 3492–3497.

(15) Frank, M.; Andersson, S.; Libuda, J.; Stempel, S.; Sandell, A.; Brena, B.; Giertz, A.; Brühwiler, P. A.; Bäumer, M.; Mårtensson, N.; Freund, H.-J. *Chem. Phys. Lett.* **1997**, *279*, 92–99.

(16) Henry, C. R. *Surf. Sci. Rep.* **1998**, *31*, 231–326.

(17) Haruta, M. *Catal. Today* **1997**, *36*, 153–166.

(18) Valden, M.; Lai, X.; Goodman, D. W. *Science* **1998**, *281*, 1647–1650.

(19) Allers, K.-H.; Pfnür, H.; Feulner, P.; Menzel, D. *J. Chem. Phys.* **1994**, *100*, 3985–3998.

(20) Matsushima, T. *Surf. Sci.* **1983**, *127*, 403–423.

this case, oxygen atoms that are produced during the dissociation process of O_2 on the surface oxidize carbon monoxide. In such a mechanism oxygen atoms react with CO before they reach the energy minimum of the oxygen−surface interaction potential, and therefore no additional activation for the actual oxidation step is needed.[19] A second reaction channel on Pt(111) involves chemisorbed oxygen atoms, which oxidize adsorbed CO at temperatures higher than 200 K. This mechanism can also be observed on low-coordinated platinum sites, e.g., the ones on a Pt(355) surface,[22,23] and the oxidation temperature of this mechanism is sensitively dependent on the character of the reactive site.[22] In addition to this rather detailed picture of the energetics of the process, a complex spatial and temporal pattern of this seemingly simple reaction was discovered.[24] Studies on Pt(100) and Pt(110) surfaces revealed a complicated modification of the overall CO oxidation caused by an adsorption-induced change in the surface structure, which leads to oscillations during the reaction.[25] Real catalysts for the oxidation of CO consist of highly dispersed metal particles on refractory metal oxides.[26−28] Besides changes in the reactivity due to the existence of different crystalline facets on Pt particles[29,30] a few nanometers in size, the very small clusters investigated in this work consisting only of a few atoms show pronounced size effects in their catalytic behavior. This is caused by the changing coordination number in different geometric structures and/or the changing electronic structures as a function of cluster size. The observed overall size-dependent reactivity can be rationalized with changes in the cluster's morphology and within simple frontier orbital considerations, which suggest that the changing energy match between the π_g^* antibonding orbital of the oxygen molecule and the cluster electronic states is decisive for this catalytic reaction.

2. Experimental Section

The Pt clusters are generated with a high-frequency laser evaporation source, producing high currents of singly positively charged clusters. In this setup the output (355 nm) of a Nd:Yag laser is focused on a rotating Pt target disk. A helium pulse thermalizes the produced metal plasma, and the clusters are grown by nucleation when the helium−metal vapor undergoes supersonic expansion. Subsequently they are size-selected by a quadrupole mass filter and deposited onto a magnesium oxide thin film.[31] The total energy of the deposition process is composed of the kinetic energy of the cluster ($E_{kin} < 0.2$ eV/atom[31]), the involved chemical binding energy between the cluster and the MgO surface (~1.4 eV per interacting atom[32]), and a negligible Coulomb interaction of the incoming cluster ion and its induced polarization charge on the oxide film surface. Consequently, as the kinetic energies of the impinging clusters correspond to soft-landing conditions ($E_{kin} \leq 1$ eV) [33,34] and as the total energy gained upon the deposition is at least a factor of 2 smaller than the binding energy of the investigated Pt clusters ranging from 2.5 to 5 eV,[35,36] fragmentation of the clusters

is excluded.[37] Upon impact the cluster ions are neutralized either on defect sites (F, F^+ centers) or by charge tunneling through the thin MgO films. We deposited only 0.14−0.22% of a monolayer (ML) of Pt clusters (1 ML $= 2.2 \times 10^{15}$ clusters/cm^2) at 90 K to land them isolated on the surface and to prevent agglomeration on the MgO films.[38] The support is prepared in situ for each experiment by epitaxially growing thin films on a Mo(100) surface by evaporating magnesium in a $^{16}O_2$ background.[39] To obtain identical conditions for the study of the catalytic reactivity of the different Pt clusters, we first exposed the prepared model catalysts by a calibrated molecular beam doser at 90 K to an average of 20 $^{18}O_2$ molecules per Pt atom. This results in saturation coverages on the clusters, as evidenced experimentally.[40] Subsequently, we exposed the system to the same amount of $^{12}C^{16}O$. This is crucial, as it is well-known from single-crystal studies that the initial amount of oxygen and CO on the surface and the ratio of these molecules during oxidation may influence the reactivity.[19,22,23,41] Isotopically labeled $^{18}O_2$ molecules were used to disentangle the CO_2 production on the cluster surface from an eventual catalytic oxidation of CO involving MgO substrate oxygen atoms. In a temperature-programmed reaction (TPR) experiment we then detected the differently labeled CO_2 molecules, which are catalytically produced on the surface of the clusters. The catalytic action is determined by integrating the TPR signal of the CO_2 molecule and normalizing to the number of deposited clusters. For this procedure the mass spectrometer has been calibrated using the known amount of desorbing CO from a Mo(100) single crystal[42] and taking into account its different sensibilities for CO and CO_2. The number of deposited clusters was obtained by integrating the measured ion current on the substrate over the deposition time. In addition, for selected Pt cluster sizes Fourier transform infrared (FTIR) studies have been performed to detect catalytically active sites on the cluster surface via CO vibrational frequencies. Finally we note that the prepared MgO(100) films do not catalyze the oxidation of CO.

3. Results

Figure 1 shows the TPR spectra for the CO oxidation on supported Pt_n ($8 \leq n \leq 20$) clusters. Since only CO_2 molecules containing one isotopically labeled ^{18}O atom are detected, oxygen is dissociated prior to or during the catalytic oxidation of CO. Thus, already these small Pt particles are catalytically active. Remarkably, each cluster size reveals different oxidation temperatures, labeled α, β_1, and β_2, and a different catalytic activity as reflected in the different ion signal intensities. The main CO_2 production, labeled β_1, occurs at temperatures between 200 and 400 K. For Pt_{15} to Pt_{20} the CO_2 production is also detected at temperatures around 150 K, labeled α, while Pt_{20} clusters display an additional reaction at 460 K, labeled β_2. The different oxidation temperatures (peaks α, β_1, and β_2 in Figure 1) indicate different catalytic processes occurring on different active sites on the Pt clusters. Results of FTIR

(21) Ohno, Y.; Matsushima, T. *Surf. Sci.* **1991**, *241*, 47−53.

(22) Xu, J.; Yates, J. T., Jr. *J. Chem. Phys.* **1993**, *99*, 725−732.

(23) Szabò, A.; Henderson, M. A.; Yates, J. T., Jr. *J. Chem. Phys.* **1992**, *96*, 6191−6201.

(24) Ertl, G.; Norton, P. R.; Rüstig, J. *Phys. Rev. Lett.* **1982**, *49*, 177.

(25) Rotermund, H. H. *Surf. Sci. Rep.* **1997**, *29*, 265−364.

(26) Freund, H. J. *Angew. Chem., Int. Ed. Engl.* **1997**, *36*, 452−475.

(27) Goodman, D. W. *Surf. Rev. Lett.* **1995**, *2*, 9−24.

(28) Goodman, D. W. *Chem. Rev.* **1995**, *95*, 523.

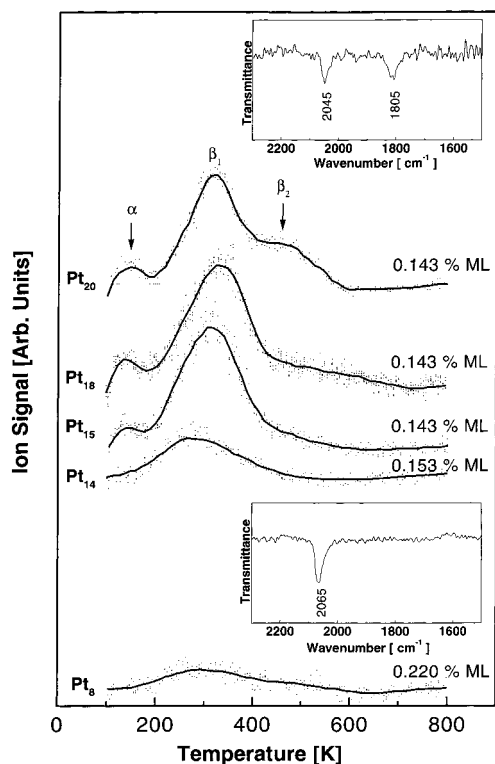(29) Duriez, C.; Henry, C. R.; Chapon, C. *Surf. Sci.* **1991**, *253*, 190.

(30) Henry, C. R.; Chapon, C.; Duriez, C. *Surf. Sci.* **1991**, *253*, 177.

(31) Heiz, U.; Vanolli, F.; Trento, L.; Schneider, W.-D. *Rev. Sci. Instrum.* **1997**, *68*, 1986.

(32) Yudanov, I.; Pacchioni, G.; Neyman, K.; Rösch, N. *J. Phys. Chem.* **1997**, *101*, 2786−2792.

(33) Bromann, K.; Félix, C.; Brune, H.; Harbich, W.; Monot, R.; Buttet, J.; Kern, K. *Science* **1996**, *274*, 956−958.

(34) Cheng, H.-P.; Landman, U. *J. Phys. Chem.* **1994**, *98*, 3527.

(35) Yang, S. H.; Drabold, D. A.; Adams, J. B.; Ordejon, P.; Glassford, K. *J. Phys.: Condens. Matter* **1997**, *9*, L39−L45.

(36) Sachdev, A.; Masrl, R. I.; Adams, J. B. *Z. Phys. D: At., Mol. Clusters* **1993**, *26*, 310−312.

(37) A direct experimental proof of this reasoning can be given, e.g., by local probe methods.

(38) We note that deposition of Cu atoms with an energy of 3−6 eV at a coverage of 4% of a monolayer exhibits the same atomic-like features in electron energy loss spectra as were observed for vapor-deposited Cu atoms (see: Schaffner, M.-H.; Patthey, F.; Schneider, W.-D.; Pettersson, L. G. M. *Surf. Sci.* **1998**, *450*, 402−404). Since the calculated binding energy (32) of Cu on MgO (0.3 eV) compared to Pt on MgO (1.36 eV) is a factor of about 4 smaller, migration of Pt clusters can be safely excluded.

(39) Wu, M. C.; Corneille, J. S.; Estrada, C. A.; He, J.-W.; Goodman, D. W. *Chem. Phys. Lett.* **1991**, *182* (5), 472.

(40) For Pt_8 and Pt_{20} the CO oxidation was investigated as a function of the initial oxygen coverage. The results show saturation of the CO_2 production at an exposure of 20 molecules per deposited atom for both sizes.

(41) Rar, A.; Matsushima, T. *Surf. Sci.* **1994**, *318*, 89−96.

(42) Zaera, F.; Kollin, E.; Gland, J. L. *Chem. Phys. Lett.* **1985**, *121* (4/5), 464.

3216   *J. Am. Chem. Soc., Vol. 121, No. 13, 1999*

Heiz et al.

Figure 1. Catalytic CO_2 formation for different cluster sizes from temperature-programmed reaction experiments. Cluster coverage is expressed in percent of a monolayer, where one monolayer corresponds to $2.2 \times 10^{15}/cm^2$. Cluster coverage is scaled with an estimated area covered by each cluster size. Different CO_2 formation mechanisms (α, β_1, β_2) are labeled according to single-crystal studies. The inset shows measured vibrational frequencies of CO adsorbed on clean deposited Pt_{20} (above) and Pt_8 (below) clusters.
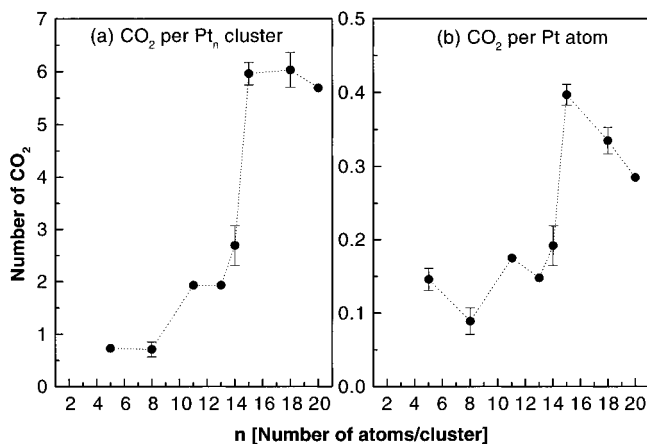
Figure 2. (a) Total number of catalytically produced CO_2 molecules as a function of cluster size. (b) Total number of produced CO_2 molecules per atom as a function of cluster size.

experiments, displayed in the inset of Figure 1, support this assumption, showing only one CO absorption frequency (2065 cm^{-1}) for Pt_8 but two absorption frequencies (2045 and 1805 cm^{-1}) for Pt_{20}.

Expressing the catalytic activity of the monodispersed Pt clusters as the number of catalyzed CO_2 molecules per cluster (Figure 2a) and per atom (Figure 2b), we note that the CO_2 production increases nonlinearly with cluster size. Up to Pt_8 less than one CO_2 molecule per cluster is formed (Figure 2a). The reactivity increases abruptly in going from Pt_8 to Pt_{15}, on which about 6 CO molecules are oxidized. For the oxidation of CO per atom (Figure 2b) a maximum of 0.4 and minimum of
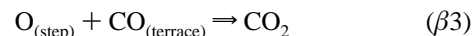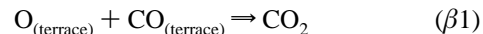
0.1 are observed for Pt_{15} and Pt_8, respectively. In addition the reactivity shows a local decrease for Pt_{13} clusters.

4. Discussion

To rationalize these observations, a comparison with the catalytic oxidation of CO on Pt single-crystal surfaces is elucidating. Two main mechanisms have been observed. (I) On Pt(111) terrace sites the reaction α has been found at 160 K

$$O_2^- + 2CO_{(terrace)} \rightleftharpoons 2CO_2 \qquad (\alpha)$$
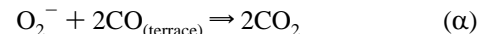
involving hot oxygen atoms.[19,43] On a stepped Pt(355) surface the reactions β at 290, 350, and 200 K have been identified, respectively.[22]

$$O_{(terrace)} + CO_{(terrace)} \rightleftharpoons CO_2 \qquad (\beta 1)$$

$$O_{(step)} + CO_{(step)} \rightleftharpoons CO_2 \qquad (\beta 2)$$

$$O_{(step)} + CO_{(terrace)} \rightleftharpoons CO_2 \qquad (\beta 3)$$

Since the oxidation temperatures on size-selected Pt clusters are in a similar range, we identify the reaction sites accordingly. The throughout presence of the β-mechanism indicates dissociation of O_2 on all cluster sizes. The α mechanism is only observed for larger clusters, Pt_{15} to Pt_{20}, implying that oxygen is adsorbed molecularly in an ionic state only on these species. Thus, the presence of higher coordinated and therefore less reactive atoms on the cluster (as on single-crystal terraces) is suggested. This is not unexpected as the average coordination number of atoms in clusters is increasing with size. If we now compare these reactivities per atom with the ones obtained from Pt single-crystal surfaces, we have to consider that the reactivity converges to zero for the latter case because of their small surface-to-bulk atom ratio. Nevertheless, on Pt(112) a reactivity per Pt surface atom of <0.2 has been determined,[23] which is more than a factor of 2 smaller than the one found for Pt_{15} (see Figure 2b).

To understand this size-dependent reactivity, the geometric and electronic structures of each Pt cluster have to be considered. Local density functional (LDF) calculations (in a non-self-consistent Harris functional version) showed that free clusters up to Pt_6 are planar,[35] and it is likely that they remain planar on MgO as additional energy is gained by the cluster substrate interaction for 2-dimensional structures in comparison to 3-dimensional structures. The optimized geometry of Pt_{10} with C_s point group symmetry has 10 atoms arranged into three layers resembling (111) planes, as obtained by using DFT calculation including relativistic effects.[44] Self-consistent LDF[45] and embedded atom method (EAM)[36] calculations predict three-dimensional structures for Pt_{13} clusters with cuboctahedron symmetry (O_h) and a highly asymmetric, irregular, and defected structure, respectively. The larger clusters Pt_n ($n > 13$) are considered to be 3-dimensional.[36] The change in the measured reactivity, expressed in the number of produced CO_2 per cluster (Figure 2a), correlates with the predicted morphological transition from 2- to 3-dimensional structures for Pt cluster sizes between Pt_6 and Pt_{10}. It is interesting to note that Pt_{13} shows a local minimum in the reactivity per atom (Figure 2b), with Pt_{13} being the first atomic-shell closing of both icosahedral and cuboctahedral structures. However, in addition to morphological

(43) Zambelli, T.; Barth, J. V.; Wintterlin, J.; Ertl, G. *Nature* **1997**, *390*, 495−497.

(44) Watwe, R. M.; Spiewak, B. E.; Cortright, R. D.; Dumesic, J. A. *Catal. Lett.* **1998**, *51*, 139−147.

(45) Watari, N.; Ohnishi, S. *J. Chem. Phys.* **1997**, *106*, 7531−7540.
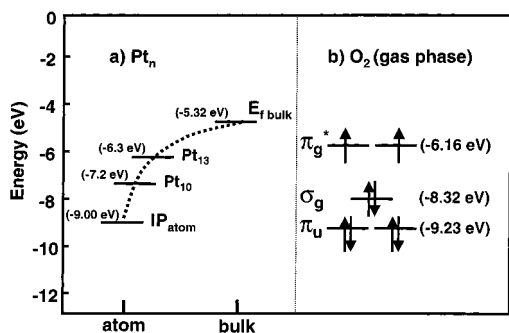
Figure 3. Energy diagram of the relevant electronic states for the oxygen dissociation for gas-phase clusters and free oxygen. The clusters' HOMOs are between the atomic limit (-9.00 eV) and the bulk limit (-5.32 eV). Included are the calculated positions of the centers of the d-bands for Pt_{10} (-7.2 eV)[44] and Pt_{13} (-6.3 eV).[45] Dotted line: classical conductive droplet model[50] (the expected fine structure of the ionization potentials observed for small metal clusters[50,51] is not taken into account). Dissociation is favored if the energy of the cluster's HOMO is close to the antibonding π_g^* state of oxygen.

changes as a function of cluster size, the different electronic structure of the Pt_n clusters is important in understanding their catalytic behavior. As shown above, the dissociation of O_2 is the first step in this catalytic reaction and determines the measured reactivity, which is the number of produced CO_2 molecules per cluster or per deposited atom, respectively. Therefore, we concentrate on this process, and in the absence of theoretical model calculations even for CO oxidation on small Pt clusters, we analyze qualitatively the chemical interaction in terms of the frontier orbitals of the oxygen molecule and the Pt cluster (see Figure 3).[46] Here we simply replace the molecule−single crystal surface interaction by the molecule−cluster surface interaction. For the oxygen molecule the electronic states of interest are the bonding, fully occupied π_u and σ_g and the antibonding, half-occupied π_g^* orbitals. Providing there exists a resonance (energetically and symmetrically) between one of these orbitals and the cluster's density of state (DOS), adsorption and dissociation of O_2 is possible.[46] As shown by density functional theory (DFT) calculations the d-band position is the most decisive parameter, when describing molecule−surface bonding.[47] Fragmentation occurs when there is enough back-donation from the clusters into the antibonding π_g^* state or a

sufficient donation from the π_u or σ_g orbital into the cluster.[48] Both processes reduce the bond order of oxygen. The energies of the fragment orbitals are -9.23, -8.32, and -6.1 eV for π_u, σ_g, and π_g^*, respectively.[46] On the other hand, by changing the cluster size, the energy of the highest occupied orbitals (HOMO) of the clusters, associated with the energy of the center of the d-band,[44,45] can be tuned from -9.0 eV, the ionization potential (IP) of the atom, to -5.32 eV, the Fermi energy of bulk platinum (Figure 3).[49] Now the increase in the catalytic activity from Pt_8 to Pt_{15} can be correlated with the decrease of the IP and the change in the position of the center of the d-band with increasing cluster size and the concomitant enhanced resonance with the antibonding π_g^* state of O_2. The maximum reactivity for Pt_{15} suggests that the resulting back-donation is largest for this cluster. Increasing the cluster size further lowers the cluster's HOMO even more and may result in a weaker resonance with the antibonding π_g^* state of O_2, as the HOMO's energy passes the energy of this antibonding state. For the very small particles this back-donation is small as the energy mismatch of the cluster's HOMO and π_g^* is large (Figure 3).

5. Conclusion

To summarize, we have shown for a single-pass heating cycle that every single Pt atom composing the supported cluster counts for the catalytic activity of the oxidation of carbon monoxide. Surprisingly, simple geometric and molecular orbital arguments seem to be sufficient to describe the general trend of the observed catalytic activity with cluster size. The prospect of tuning catalytic processes as a function of cluster size, a long-sought goal in heterogeneous catalysis, is a little less remote.

(46) Chen, A. W. E.; Hoffmann, R.; Ho, W. *Langmuir* **1992**, *8*, 1111−1119.

(47) Hammer, B.; Nielsen, O. H.; Nørskov, J. K. *Catal. Lett.* **1997**, *46*, 31−35.

(48) Hoffman, R. *Solids and Surfaces: A Chemist's View of Bonding in Extended Structures*; VCH Verlagsgesellschaft, GmbH: Weinheim, 1988.

(49) The interaction of the supported clusters with the MgO substrate is neglected in this simple picture.

(50) Schumacher, E.; Blatter, F.; Frey, M.; Heiz, U.; Röthlisberger, U.; Schär, M.; Vayloyan, A.; Yeretzian, C. *Chimia* **1988**, *42*, 357−376.

(51) Heiz, U.; Vayloyan, A.; Schumacher, E. *J. Phys. Chem.* **1996**, *100*, 15033−15040.